# FOXD1 promotes chemotherapy resistance by enhancing cell stemness in colorectal cancer through β-catenin nuclear localization

WEN-QING FENG*, YU-CHEN ZHANG*, HAN GAO*, WEN-CHANG LI, YI-MING MIAO, ZI-FENG XU, ZHUO-QING XU, JING-KUN ZHAO, MIN-HUA ZHENG, YA-PING ZONG and AI-GUO LU

Department of General Surgery, Ruijin Hospital, Shanghai Jiao Tong University School of Medicine, Shanghai 200020, P.R. China

Received January 18, 2023; Accepted April 20, 2023

DOI: 10.3892/or.2023.8571

**Abstract.** Forkhead box D1 (FOXD1) serves a critical role in colorectal cancer (CRC). FOXD1 expression is an independent prognostic factor in patients with CRC; however, the molecular mechanism and signaling pathway of FOXD1 that regulates cell stemness and chemoresistance has not been fully characterized. The aim of the present study was to further validate the effect of FOXD1 on the proliferation and migration of CRC cells, and to delve into the possible potential of FOXD1 in the clinical treatment of CRC. The effect of FOXD1 on cell proliferation was assessed using Cell Counting Kit 8 (CCK-8) and colony formation assays. The effect of FOXD1 on cell migration was assessed by wound-healing and Transwell assays. The effect of FOXD1 on cell stemness was assessed by spheroid formation *in vitro* and limiting dilution assays *in vivo*. The expression of stemness associated proteins, leucine rich repeat containing G protein-coupled receptor 5 (LGR5), OCT4, Sox2 and Nanog, and epithelial-mesenchymal transition associated proteins, E-cadherin, N-cadherin and vimentin, were detected by western blotting. Proteins interrelationships were assessed by a co-immunoprecipitation assay. Oxaliplatin resistance was assessed using CCK-8 and apoptosis assays *in vitro*, and using a tumor xenograft model *in vivo*. By constructing FOXD1 overexpression and knockdown stably transfected strains of colon cancer cells, it was revealed that the overexpression of FOXD1 increased CRC cell stemness and chemoresistance. By contrast, knockdown of FOXD1 produced the opposite effects. These phenomena were caused by the direct interaction between FOXD1 and β-catenin, thus promoting its nuclear translocation and the activation of downstream target genes, such as LGR5 and Sox2. Notably, inhibition of this pathway with a specific β-catenin inhibitor (XAV-939) could impair the effects induced by the overexpression of FOXD1. In summary, these results indicated that FOXD1 may promote cell stemness and the chemoresistance of CRC by binding directly to β-catenin and enhancing β-catenin nuclear localization; therefore, it may be considered a potential clinical target.

## Introduction

Colorectal cancer (CRC) is the third most prevalent and deadly malignant disease worldwide (1). Despite improvements in diagnosis and treatment in recent years, the average survival time of patients with advanced CRC remains poor, with distant invasion and metastasis accounting for 90% of CRC-related deaths (2).

Forkhead box (FOX) proteins, which regulate a wide variety of cellular pathways during cancer development, including the TGF-β cascade, Wnt pathway, Sonic-Hedgehog pathway and MAPK pathway, are a superfamily of evolutionarily conserved transcription factors (3). Accumulating evidence has indicated that FOX proteins may act as critical nodes in cellular networks, allowing cross-talk among biological pathways (4,5). FOXD1 is a member of the FOX family (6). In our previous study, the expression levels of FOXD1 were examined using immunohistochemical staining, and the association between FOXD1 expression and clinicopathologic features was assessed. Notably, FOXD1 expression was revealed to be an independent prognostic factor in patients with CRC (7). It has also been demonstrated that FOXD1 serves a key role in the development, progression and metastasis of numerous malignancies (8). For example, high FOXD1 expression has been reported to be associated with poor survival in non-small cell lung cancer (9). Furthermore, FOXD1 promotes breast cancer growth and resistance to chemotherapeutic agents (10). By contrast, knockdown of FOXD1 has been shown to attenuate CRC cell proliferation, migration and invasion (11).

*Correspondence to:* Professor Ai-Guo Lu or Dr Ya-Ping Zong, Department of General Surgery, Ruijin Hospital, Shanghai Jiao Tong University School of Medicine, 197 Ruijin 2nd Road, Huangpu, Shanghai 200020, P.R. China
E-mail: luaiguo1965@163.com
E-mail: angela_zyp@126.com

*Contributed equally

*Key words:* forkhead box D1, colorectal cancer, stemness, chemotherapy resistance, β-catenin

Reports on the relationship between FOXD1 and tumors has resulted in FOXD1 now being recognized as a potential target for anticancer therapy. However, the mechanisms underlying the effects of FOXD1 on promoting cell stemness and chemotherapy resistance remain to be investigated.

Cancer stem cells (CSCs) are a characteristic class of cells that are capable of self-renewal in tumors with anti-apoptosis, asymmetric cell division and high metastatic capacity (12), and genetic heterogeneity, which has been reported to be associated with poor prognosis of cancer (13). Given these characteristics, research on cancer cell stemness has great clinical relevance: CSCs show more resistance to conventional chemotherapeutic agents used for anticancer treatment (14), and CSCs undergo epithelial-mesenchymal transition (EMT), which is responsible for tumor recurrence and metastasis (15). Particularly from a clinical point of view, the study of the molecular regulatory mechanisms of CSCs is crucial for the development of effective treatments to improve patient prognosis. Therefore, these aforementioned findings on CSCs may provide a novel direction in the study of CRC.

The aim of the present study was to further validate the effect of FOXD1 on the proliferation and migration of CRC cells, and to delve into the possible potential of FOXD1 in the clinical treatment of CRC.

## Materials and methods

*Access to public databases*. The data analyzed in the present study are publicly available in The Cancer Genome Atlas (TCGA; http://cancergenome.nih.gov/). Pan-cancer analysis was performed to assess the differences in FOXD1 expression between tumor tissue and paired normal tissue from 33 types of cancer in TCGA database. Data from 111,60 patients were examined using Gene Expression Profiling Interactive Analysis (http://gepia.cancer-pku.cn/). A total of 537 CRC tumor tissue samples downloaded from TCGA were divided into high and low FOXD1 expression groups (247 patients/group) based on the median geometric mean expression value.

*Specimens and immunohistochemistry*. CRC tumor tissues and paired normal tissues (>5 cm distance from the margin of the resection) were collected during surgery and used to generate a CRC tissue microarray (TMA). The TMA was generated by Shanghai Outdo Biotech Co., Ltd. Continuous sections (4 $\mu$m) were cut from the paraffin-embedded TMA. A total of 131 post-surgical patients with CRC who underwent surgery between 2009 and 2012 at the Shanghai Ruijin Hospital (Shanghai, China) were enrolled in this retrospective study. The patients were aged 35-80 years (average age, 60.8±2.7 years) and there was a male/female sex ratio of 0.926. Patients who received preoperative treatment, such as radiotherapy or chemotherapy, were excluded from the study. Human tissue collection and experiments using human tissue were approved by the Institutional Review Board of Ruijin Hospital Ethics Committee (institutional approval no. 2018-07-015; Shanghai Jiao Tong University School of Medicine). The tissue was fixed at room temperature in 10% formaldehyde for 30-60 min. The tissue was then sequentially dehydrated in ethanol solutions and washed with xylene, before being embedded in paraffin (4 $\mu$m). The sections were permeabilized with 0.2% Triton X-100 and blocked with 3% bovine serum albumin (BSA; Gibco; Thermo Fisher Scientific, inc.) for 30-60 min at room temperature. Subsequently, the slides were incubated with a primary antibody against FOXD1 (1:200; cat. no. A20240; ABclonal Biotech Co., Ltd.) at 4˚C overnight, followed by a 30-60 min incubation with a HRP Goat Anti-Rabbit IgG (H+L) secondary antibody (1:200; cat. no. ab205718; Abcam) at room temperature. Tissues were counterstained with hematoxylin for 5-10 min at room temperature and were observed under a light microscope.

*Immunohistochemical score*. Two independent pathologists scored the intensity of immunohistochemical staining of FOXD1 in tumor tissues according to a semi-quantitative immunoreactivity scoring system. The percentage of immunoreactive cells was scored as follows: 0, 0%; 1, 1-10%; 2, 11-50%; 3, 51-80%; and 4, >80%. The staining intensity was scored as follows: 0, No staining; 1, weak staining; 2, moderate staining; 3, intense staining. These values were multiplied together to provide a single score ranging between 0 and 12 for each case.

*Cell culture and reagents*. A total of seven different CRC cell lines were used in the present study: SW620, HT29, SW480, HCT116, LOVO, DLD1 and RKO. All human CRC cell lines were purchased from the American Type Culture Collection and stored at the Shanghai Institute of Gastrointestinal Surgery. All CRC cell lines were cultured in RPMI-1640 medium (Dalian Meilun Biology Technology Co., Ltd.) supplemented with 10% newborn calf serum (NBS; Gibco; Thermo Fisher Scientific, Inc.). The cells were cultured at 37˚C in a 5% $CO_2$ environment.

The following primary antibodies were used: Rabbit anti-FOXD1 (cat. no. A20240; ABclonal Biotech Co., Ltd.), rabbit anti- histone H3 antibody (cat. no. A2348; ABclonal Biotech Co., Ltd.), rabbit anti-E-cadherin (cat. no. 3195T; Cell Signaling Technology, Inc.), rabbit anti-N-cadherin (cat. no. 13116T; Cell Signaling Technology, Inc.), rabbit anti-vimentin (cat. no. ab92547; Abcam), rabbit anti-β-catenin (cat. no. ab32572; Abcam), rabbit anti-leucine rich repeat containing G protein-coupled receptor 5 (LGR5) (cat. no. ab75850; Abcam), rabbit anti-Oct4 (cat. no. ab19857; Abcam), rabbit anti-Sox2 (cat. no. ab92494; Abcam), rabbit anti-Nanog (cat. no. ab109250; Abcam) and mouse anti-GAPDH (cat. no. ab8245; Abcam).

XAV-939 (MedChemExpress) is a potent and cell-permeable small molecule inhibitor that selectively inhibits tankyrase activity and thereby suppresses Wnt/β-catenin signaling pathway-mediated transcription. CRC cells were treated with 2 nmol/l XAV-939 at 37˚C for 24 h.

*Generation of stable gene-overexpressing and knockdown cells*. Generation of stable gene-overexpressing and knockdown cells was performed using standard methods (16). The EF1a-GFP/Puro-FOXD1 lentiviral plasmid (lentiviral vector, LV5; Shanghai GenePharma Co., Ltd.) and short hairpin (sh)RNA pGLV-h1-GFP/Puro-shFOXD1 lentiviral plasmid (lentiviral vector, LV3; Shanghai GenePharma Co., Ltd.) were used to generated gene-overexpressing and knockdown cells. The 2nd generation system was used. Briefly, 293T cells (American Type Culture Collection; stored at the Shanghai

Institute of Gastrointestinal Surgery) were transfected with 10 $\mu$g lentiviral plasmid in a 10-cm dish; the ratio used for the lentivirus, packaging and envelope plasmids was 4:3:1. Cells were transfected for 48 h at 37˚C using Lipofectamine® 2000 transfection reagent (cat. no. 11668030; Invitrogen; Thermo Fisher Scientific, Inc.). Polyethylene glycol was used to collect the lentiviral particles and a multiplicity of infection of 5 was used to infect the CRC cells for 72 h at 37˚C, and there was a 72-h interval between transduction and subsequent experimentation. Puromycin was used for selection (8 $\mu$g/ml) and for maintenance (5 $\mu$g/ml) of transduced cells. The targeting sequence of shRNA-FOXDA (shFOXD1) was 5'-TGTCCA GTGTCGAGAACTTTA-3'. Briefly, $3x10^5$ cells were seeded into each well of a six-well plate 1 day before transfection. When the cells reached 70% confluence, the culture medium was replaced with fresh normal medium. In each well, 50 $\mu$l primary lentivirus solution was diluted in 400 $\mu$l normal medium and polybrene was added at a final concentration of 5 $\mu$g/ml. Subsequently, the mixture was added to each well. After 24 h, the medium in each well was replaced. A total of 48 h after transfection, puromycin was used to screen stable cell clones, and 72 h after transfection, the overexpression and interfering effect of these vectors/shRNAs were evaluated by western blotting. Empty vectors were used as a control for sh-FOXD1-induced knockdown and FOXD1 overexpression.

*Western blotting*. Western blot analysis was performed using standard methods (16). Proteins were extracted from tissues and cells using RIPA Lysis Buffer (MedChemExpress). Briefly, 50 $\mu$g protein/lane was separated by SDS-PAGE on 12.5% gels and transferred to polyvinylidene fluoride membranes. The membranes were blocked with 5% BSA for 2 h at room temperature and then incubated with primary antibodies (1:2,000) at 4˚C overnight. Subsequently, the membranes were incubated with the corresponding secondary antibody Goat Anti-Rabbit IgG H&L (HRP) (1:10,000; ab6721; Abcam) at room temperature for 1 h and the protein bands were visualized using an enhanced chemiluminescence detection system (Amersham; Cytiva). ImageJ (version 1.8.0; National Institutes of Health) was used for semi-quantification.

NE-PER Nuclear Extraction Reagent (Thermo Fisher Scientific, Inc.) was used to isolate and extract nuclear proteins, respectively. Specific detailed steps were performed as described previously (17).

*Wound-healing and Transwell assays*. CRC cells ($1x10^5$/well) were cultured in 6-well plates. After 16 h, the culture medium was replaced with low-serum fresh medium (2%). After cells had reached 90% confluence, the cells in each well were scratched using a 200-$\mu$l pipette tip to create consistent wounds. Specific detailed steps were performed as described previously (18). Images of the scratch areas were captured under an inverted light microscope at 0 and 24 h at 37˚C. The assays were repeated three times. Wound width was calculated as the average distance between the edges of the scratch. Relative migration distance=final wound width/initial wound width x100.

Migration was examined using Boyden chamber plates (pore size, 8 $\mu$m). Cells ($1x10^5$) were resuspended in medium without NBS (200 $\mu$l) and were added to the upper chamber, with medium containing 20% NBS added to the lower chamber. After 24 h at 37˚C, the cells were fixed with 4% paraformaldehyde for 20 min at room temperature and stained with 0.1% crystal violet staining solution for 5 min at room temperature, and six randomly selected areas were examined under a light microscope. The cell numbers were counted and statistically analyzed.

*Tumor sphere formation*. The cells were detached from culture flasks with 0.25% trypsin and suspended in sphere formation medium (50 ml DMEM/F12 containing 100 mg/ml EGF, 100 mg/ml bFGF and 1 ml B-27® Supplement; Gibco; Thermo Fisher Scientific, Inc.). The cells were then filtered into a single-cell suspension and seeded. Cells (200 cells/well) were seeded in ultra-low adherence 96-well plates (Corning, Inc.) and were cultured in NBS-free medium for 14 days and the spheroids were observed under a light microscope.

*Cell Counting Kit-8 (CCK-8) and colony formation assays*. Cell viability was examined using a CCK-8 assay (Sevenbio). Cells were seeded in 96-well plates at a density of $4x10^3$ cells/well in 200 $\mu$l medium for 1-5 days at 37˚C. The absorbance was detected at 450 nm after the cells were treated with 10% CCK-8 at 37˚C for 2 h. Cell proliferation was calculated as a ratio of optical density values of drug-treated samples to those of controls.

Colony formation was examined to determine transformation and anchorage-independent growth (19). The cells were detached from culture flasks with 0.25% trypsin and suspended in sphere formation medium. The cells were then filtered into a single-cell suspension and seeded. Cells (1,000 cells/well) were then seeded in 6-well plates (Corning, Inc.), cultured for 14 days at 37˚C, and colonies (>50 cells and >0.3 mm in diameter) were counted and images were captured.

*Immunofluorescence (IF) staining*. Cells ($1x10^4$/well) were cultured on coverslips in 24-well plates for 24 h at 37˚C, fixed with 4% formaldehyde at room temperature, blocked with 5% BSA at room temperature and permeabilized with 0.5% Triton X-100 at room temperature. Cells that adhered to coverslips were then incubated with rabbit anti-E-cadherin (1:1,000; cat. no. 3195T; Cell Signaling Technology, Inc.), rabbit anti-N-cadherin (1:500; cat. no. 13166T; Cell Signaling Technology, Inc.), rabbit anti-vimentin (1:200; cat. no. ab92547; Abcam) and rabbit anti-β-catenin (1:200; cat. no. ab32572; Abcam) primary antibodies for 4-6 h at room temperature, followed by incubation with an allophycocyanin-conjugated anti-rabbit secondary antibody (1:2,000; cat. no. F0111; Bio-Techne Corporation) for 1 h in the dark at room temperature. After incubation with DAPI (Biosharp Life Sciences) for 5 min, the cells were observed under a fluorescence microscope within 4 h.

*Co-immunoprecipitation (Co-IP)*. After transfection, cells were collected and lysed using lysis buffer (Gibco; Thermo Fisher Scientific, Inc.). After centrifugation of 10 $\mu$l precleared cell lysate at 300 x g for 15 min at 4˚C, the protein concentration in the supernatant was determined using a bicinchoninic acid assay. A total of 30 $\mu$g protein A or protein G agarose/sepharose (MilliporeSigma), and 5 $\mu$g anti-flag antibody (cat. no. F7425;

MilliporeSigma) were added to the 1 ml supernatants (protein concentration, 2 $\mu$g/$\mu$l) at 4˚C, which were subsequently incubated with a control immunoglobulin-G (IgG) (1:200; AC005; ABclonal Biotech Co., Ltd.) or anti-FOXD1 antibodies (1:200; A20240; ABclonal Biotech Co., Ltd.) in the presence of protein A or G agarose/sepharose beads overnight at 4˚C with gentle shaking. Following incubation, agarose/sepharose beads were collected and washed five times with lysis buffer. Subsequently, the complex was eluted at 100˚C for 4 min. The eluate was collected and subjected to SDS-PAGE and western blot analysis.

*Chemotherapy sensitivity assay*. Oxaliplatin is one of the most widely used chemotherapeutic agents for the treatment of CRC (20), thus the present study evaluated the sensitivity of the FOXD1-overexpressing SW620 cells, sh-FOXD1-transfected HT29 cells and control cells to this drug. The sensitivity of cells to oxaliplatin was examined using a CCK-8 assay (Dojindo Laboratories, Inc.). Briefly, several concentrations of oxaliplatin (cat. no. T0164; Shandong TopScience Biotech Co., Ltd.) (0.25, 0.5, 1, 2, 4, 8, 16, 32 and 500 $\mu$M) in RPMI-1640 medium were used, and the cells ($3x10^3$/well) were seeded in 96-well plates before being incubated with the drug for 36 h at 37˚C. The inhibition rate (%) was calculated as follows: (Absorbance control- Absorbance experiment)/Absorbance control x100.

To evaluate the resistance of SW620 cells overexpressing FOXD1, sh-FOXD1-transfected HT29 cells and control cells, a colony formation assay was performed. Briefly, cells (1,000 cells/well) were seeded in 6-well plates (Corning, Inc.), cultured for 14 days at 37˚C and colonies were counted (>50 cells, >0.3 mm in diameter). The number of colonies in normal RPMI-1640 medium was compared with the number of colonies in RPMI-1640 medium containing 4 $\mu$M oxaliplatin. The resistance to oxaliplatin was determined by comparing the reduction in colony number(%)=(1-number of colonies after oxaliplatin treatment/number of colonies control) x100.

*Apoptosis assay*. Cell apoptosis analyses were performed using the Annexin V-fluorescein isothiocyanate (FITC)-propidium iodide (PI) apoptosis detection kit (MilliporeSigma) according to the manufacturer's instructions. Transiently transfected cells were washed with PBS and trypsinized for 3-4 min. Cells were collected by centrifugation at 300 x g for 5 min at 4˚C and washed twice with ice-cold 1X PBS. On ice, cell pellets were resuspended in 100 $\mu$l 1X Annexin binding buffer, followed by staining with Annexin V-FITC and PI for 15 min in the dark at 4˚C. Cells were collected by centrifugation at 300 x g for 5 min at 4˚C, resuspended in 500 $\mu$l 1X Annexin binding buffer, and analyzed immediately by flow cytometry. A total of 10,000 cells from each event were scanned using a FACSCalibur flow cytometer (BD Biosciences) using the standard configuration and parameters. Data from quadrants demarcating unstained cells, PI-positive cells, Annexin V-FITC-positive cells, and PI- and Annexin V-FITC-positive cells were collected and analyzed using CellQuest 3.0 software (BD Biosciences).

*Tumor xenograft and metastasis in vivo*. Male Balb/c nude mice (age, 6 weeks; weight, 20-25 g; n=60 mice, 5 mice/cage) were supplied by Phenotek Biotechnology (Shanghai) Co., Ltd. Mice were subcutaneously injected with SW620NC, SW620OE, HT29NC and HT29sh cells ($1x10^6$ cells/mouse; n=5 mice/group) to generate the SW620NC, SW620OE, HT29NC and HT29sh groups. Mice were sacrificed after 2 weeks and the subcutaneous tumors were harvested, and then measured and weighed. The maximum tumor diameter permitted was 15 mm. The mice were anesthetized with chloral hydrate (4%, 400 mg/kg mouse body weight) and sacrificed by cervical dislocation, and then their tumor tissues were collected. Subsequently, immunohistochemistry, and hematoxylin and eosin (H&E) staining of tumor tissue sections were performed.

The lung metastasis models were induced by tail vein injection ($1x10^6$ cells/mouse; n=5 mice/group). The liver metastasis models were induced by spleen injection ($1x10^6$ cells/mouse; n=5 mice/group). The lung and liver metastasis model mice were split into the following groups, depending on the cells injected: SW620NC, SW620OE, HT29NC and HT29sh groups. The mice were anesthetized with chloral hydrate (4%, 400 mg/kg mouse body weight) and sacrificed by cervical dislocation, and then their lung and liver tissues were collected after 4-6 weeks. Subsequently, H&E staining of lung and liver tissue sections was performed.

*H&E staining*. Specimens were fixed in 4% paraformaldehyde for 2-3 days at room temperature, embedded in paraffin, serially sectioned (4 $\mu$m) and stained with H&E for 5 min at room temperature. Sections were observed under a light microscope.

*Tumor stemness and oxaliplatin resistance in vivo*. Male Balb/c nude mice (age, 6 weeks; weight, 20-25 g; n=36 mice, 3 mice/cage) were supplied by Phenotek Biotechnology (Shanghai) Co., Ltd. Xenograft models were induced by subcutaneously injecting the nude mice with SW620NC, SW620OE, HT29NC and HT29sh cells (n=3 mice/group) to generate the SW620NC, SW620OE, HT29NC and HT29sh groups. The limiting dilution test refers to the subcutaneous injection of cells in different concentration gradients to construct a subcutaneous xenogeneic tumor model and can be used to test the stemness of the cells. Subgroups consisting of three different concentrations ($1x10^6$, $1x10^5$ or $1x10^4$ cells/mouse) of four different cell lines (SW620NC, SW620OE, HT29NC and HT29sh) were injected subcutaneously into mice and xenografts were measured every 2-3 days.

Male Balb/c nude mice (age, 6 weeks; weight, 20-25 g; n=24 mice, 5 mice/cage) were supplied by Phenotek Biotechnology (Shanghai) Co., Ltd. Mice were subcutaneously injected with SW620NC, SW620OE, HT29NC and HT29sh cells ($1x10^6$ cells/mouse; n=3 mice/group) to generate the SW620NC, SW620OE, HT29NC and HT29sh groups. Treatment started on day 7 after injection of stably transfected cells. Murine isotype control (PBS) or oxaliplatin (5 mg/kg) were administered intraperitoneally every second day. After completing three drug injections, the mice were sacrificed, and the subcutaneous tumors were harvested and measured. Reduction in tumor volume (%) was calculated as follows: Volume of tumor after oxaliplatin treatment/volume of tumor control x100.

*Laboratory animals*. The strain of nude mice used was Balb/c and the total number of mice used was 120. The animal study protocol was approved by the Institutional Review Board of

Ruijin Hospital Ethics Committee (institutional approval no. 2019-01-047; Shanghai Jiao Tong University School of Medicine). The temperature of the mice rearing room was 20-26˚C and the relative humidity of the rearing room was 50-60%. The light intensity of the rearing room was 15-20 lx and the mice were maintained under a 12-h light/dark cycle. The drinking water and food were sterilized and were freely available. The humane endpoints for the animal study included, but were not limited to: A tumor burden >10% body weight, tumors that ulcerate, become necrotic or infected; tumors that interfere with eating or impair ambulation. In addition, tumors were not allowed to exceed 15 mm in any one dimension.

*Statistical analysis*. All experiments were performed independently at least three times. Statistical analyses were performed using SPSS statistical software (version 26; IBM Corp.) and GraphPad Prism software (version 9; Dotmatics). The Shapiro-Wilk test was used to analyze whether quantitative variables followed a normal distribution. Normally distributed data are presented as the mean ± standard deviation, whereas non-normally distributed data are presented as the median and interquartile range. The difference between groups of normally distributed data was assessed by independent samples t-test or paired t-test, when tumor tissues and paired normal samples from the same patient were assessed, whereas the difference between two groups of non-normally distributed data was assessed by the Mann-Whitney U test. For long-term outcomes, Kaplan-Meier curves were plotted, and patients with high and low FOXD1 expression were compared using the log-rank test. $P<0.05$ was considered to indicate a statistically significant difference.

## Results

*FOXD1 expression is markedly higher in tumor tissues than in normal tissues, and high FOXD1 expression is associated with poor prognosis*. Pan-cancer analysis was performed to assess differences in FOXD1 expression between tumor tissue and paired normal tissue in 33 types of cancer. Data from 11,160 patients were obtained from TCGA database and were examined using Gene Expression Profiling Interactive Analysis. The results indicated that FOXD1 was notably upregulated in tumor tissues compared with in paired normal tissues (Fig. 1A) Furthermore, a total of 537 tumor tissue samples downloaded from TCGA were divided into high and low FOXD1 expression groups (247 patients/group) based on the median geometric mean expression value. Kaplan-Meier analysis indicated that high FOXD1 expression was associated with poor prognosis in patients with CRC (Fig. 1B). To further verify FOXD1 expression in tumor tissues, tumor tissues and matched normal tissues from 131 patients with CRC in a TMA were analyzed using immunochemistry. The FOXD1 expression in the tumor tissues was markedly higher than that in adjacent normal tissues (Fig. 1C and D). Positive expression of FOXD1 was observed in 96 (73.3%) tumor tissues, whereas positive expression was observed in only 35 (26.7%) matched normal colorectal tissues (Fig. 1D). FOXD1 protein expression in cancerous and matched noncancerous tissues was confirmed by western blot analysis (Fig. 1E and F). Subsequently, the expression levels of FOXD1 in CRC cell lines were screened, and it was revealed that SW620 cells exhibited lower levels than the other cell lines, whereas the levels in HT29 cells were higher than those in the other cell lines (Fig. 1G).

*FOXD1 promotes CRC cell proliferation, migration and invasion*. Specific lentiviral vectors expressing green fluorescent protein were transduced into SW620 and HT29 cells. Western blotting verified that FOXD1 protein expression was increased in the SW620OE group relative to the SW620NC group, and that FOXD1 protein expression was decreased in the HT29sh group relative to the HT29NC group. (Fig. 2A). The effect of FOXD1 on CRC cell proliferation was examined using the CCK-8 (Fig. 2B) and colony formation (Fig. 2C and D) assays; the results indicated that FOXD1 had a promoting effect on CRC cell proliferation. Transwell assays confirmed the more aggressive migratory potential of FOXD1-overexpressing SW620 cells, whereas sh-FOXD1 inhibited the migration and invasion of HT29 cells (Fig. 2E and F). Consistent with the aforementioned results, wound-healing assays demonstrated that FOXD1 depletion significantly inhibited scratch wound healing, whereas FOXD1 overexpression enhanced CRC cell migration (Fig. 2G and H).

*FOXD1 promotes CRC cells stemness via activated β-catenin*. Sphere formation is considered an important feature in assessing tumor cell stemness *in vitro* (17). The stemness of tumor cells is considered to have an important role in tumorigenic potential, including the ability to metastasize, form colonies and exhibit resistance to cytotoxic drugs (20). To investigate the relationship between FOXD1 and CRC stemness, the sphere formation of SW620 cells overexpressing FOXD1 and HT29 cells transduced with sh-FOXD1, as well as controls, was evaluated. Examination of the spheroid formation (Fig. 3A) revealed an increased number of spheroids in the FOXD1-overexpressing SW620 cell groups compared with that in the control cell group. In addition, sphere formation was significantly reduced in sh-FOXD1-transduced HT29 cells compared with that in control cells (Fig. 3B). Furthermore, limiting dilution assays confirmed the pro-stemness effect of FOXD1 *in vivo*; HT29 cells with FOXD1 knockdown exhibited impaired tumor initiation, whereas SW620 cells with FOXD1 overexpression exhibited enhanced tumor initiation (Fig. 3C). As the number of injected cells decreased exponentially, the differences between groups became increasingly pronounced, further demonstrating that FOXD1 could affect tumor cell stemness (Fig. 3D).

Western blot analysis demonstrated that FOXD1 overexpression promoted Sox2, Oct4, Nanog, and LGR5 expression in SW620 cells, whereas FOXD1 depletion reduced their expression in HT29 cells (Fig. 3E and F). To further examine whether FOXD1 could affect stemness through impacting β-catenin, the FOXD1-overexpressing SW620 cells were incubated with or without XAV-939, a Wnt/β-catenin inhibitor that inhibits β-catenin expression. XAV-939 markedly inhibited Sox2, Oct4, Nanog and LGR5 protein expression by suppressing Wnt/β-catenin signaling pathway-mediated transcription (Fig. 3G).

*FOXD1 modulates oxaliplatin resistance of CRC cells in vitro and in vivo*. Cell stemness is considered to be among the important potential mechanisms responsible for resistance

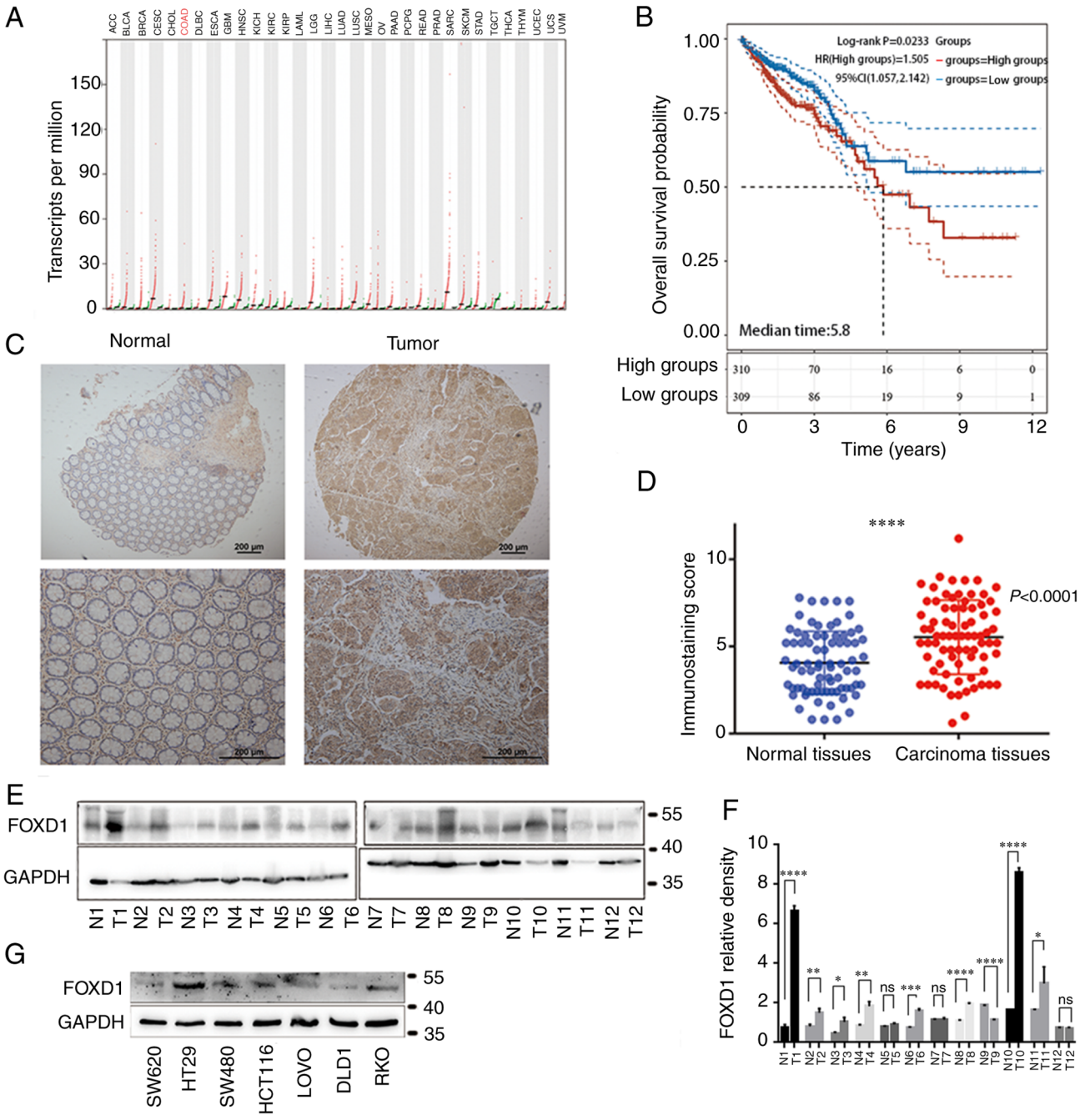


Figure 1. (A) Differentially expressed FOXD1 between tumor and normal tissues. The gene expression profile across all tumor samples and paired normal tissues is shown. Each dot represents expression in a sample. Red bar plot indicates tumor tissue, green bar plot indicates paired normal tissues. (B) Comparison of overall survival in FOXD1 high and low groups. (C) Immunohistochemical results showing high expression of FOXD1 in CRC tissues. (D) Difference in FOXD1 expression between tumor and peritumoral normal tissues is statistically significant (***P<0.001). (E) Representative western blot and (F) semi-quantification analysis of FOXD1 expression in 12 paired CRC samples. (G) FOXD1 expression in seven different colorectal cancer cell lines, SW620, HT29, SW480, HCT116, LOVO, DLD1 and RKO. FOXD1, forkhead box D1. *P<0.05, **P<0.01, ****P<0.0001. ns, not significant.

to CRC chemotherapeutic agents (15). The present study revealed that the FOXD1-overexpressing SW620 cells had higher oxaliplatin $IC_{50}$ values ($IC_{50}$=0.936) than control cells ($IC_50$=0.781), whereas sh-FOXD1-transduced HT29 cells had lower $IC_{50}$ values (IC50=4.248) than control cells ($IC_{50}$=5.017) (Fig. 4A). Although the numerical value of $IC_{50}$ seems very similar to that of the control group, the difference in percentage is ~20% and thus the relative difference is not small. Furthermore, colony formation experiments using CRC cells that were treated with oxaliplatin in normal medium revealed that FOXD1 knockdown strongly impaired CRC cell proliferation and reduced the resistance of cells to oxaliplatin. By contrast, FOXD1 overexpression promoted the proliferation and oxaliplatin resistance of SW620 cells (Fig. 4B and C). In addition, following treatment with oxaliplatin, a higher percentage of sh-FOXD1-transduced HT29 cells underwent apoptosis compared with HT29NC cells. Similarly, after treatment with oxaliplatin, a lower percentage of FOXD1-overexpressing SW620 cells underwent apoptosis compared with SW620NC cells (Fig. 4D). Necrotic cells are PI-positive, whereas apoptotic

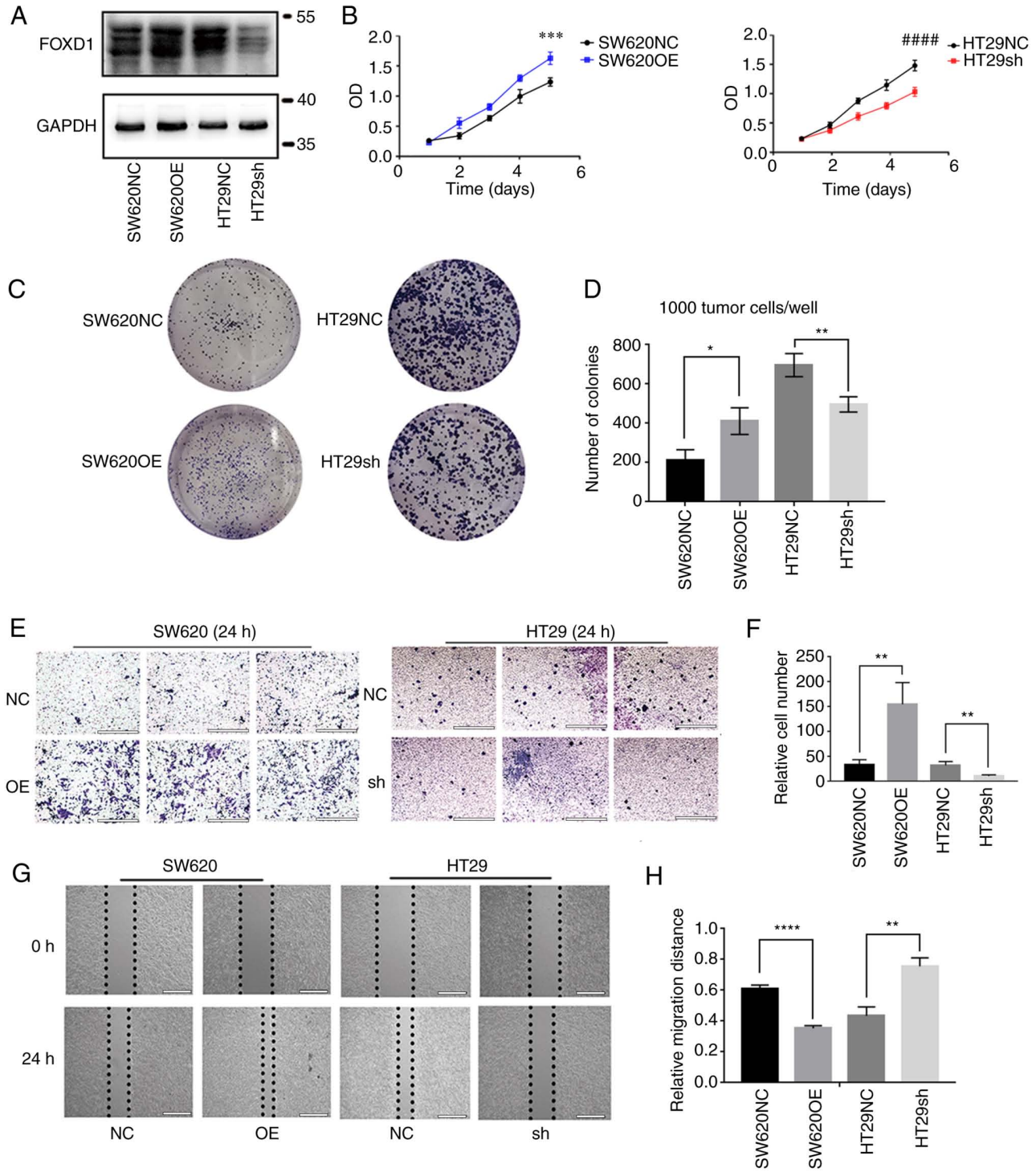


Figure 2. (A) Western blot analysis of the efficiency of FOXD1 OE and NC vectors in SW620 cells, and sh-FOXD1 and NC vectors in HT29 cells. (B) As assessed by Cell Counting Kit-8 assay, FOXD1 OE enhanced the proliferation of SW620 cells and FOXD1 depletion reduced the proliferation of HT29 cells. At day 5, the differences in absorbance between the SW620NC and SW620OE groups, and between the HT29NC and HT29sh groups were statistically significant. $^{***}$P<0.001 vs. SW620NC; $^{\#\#\#\#}$P<0.0001 vs. HT29sh. (C and D) Colony formation was increased in the SW620OE group and reduced in the HT29 sh-FOXD1 group compared with in the NC groups. (E and F) Cells migrated across the Transwell membrane filter after 24 h. Transwell assays were performed to examine the migration of FOXD1 OE SW620 cells and sh-FOXD1 HT29 cells. Scale bar, 200 $\mu$m. (G and H) Wound-healing assays of cell migration in SW620 and HT29 cells. The images of wound closure are presented at 0 and 24 h after scratching. Scale bar, 2,000 $\mu$m. $^{*}$P<0.05, $^{**}$P<0.01, $^{****}$P<0.0001. FOXD1, forkhead box D1; NC, negative control; OE, overexpression; sh, short hairpin.

cells were positive for Annexin V-FITC fluorescence. Upper and lower right quadrants were assessed.

To further investigate whether FOXD1 enhances chemoresistance *in vivo*, a chemoresistant nude mouse model was used. Nude mice bearing tumors from SW620 control cells or FOXD1-overexpressing SW620 cells, and HT29 control cells or FOXD1 knockdown HT29 cells were treated with oxaliplatin (5 mg/kg body weight; intraperitoneal injection) or PBS every other day, and the tumor size was measured after three treatments. The results showed that after FOXD1

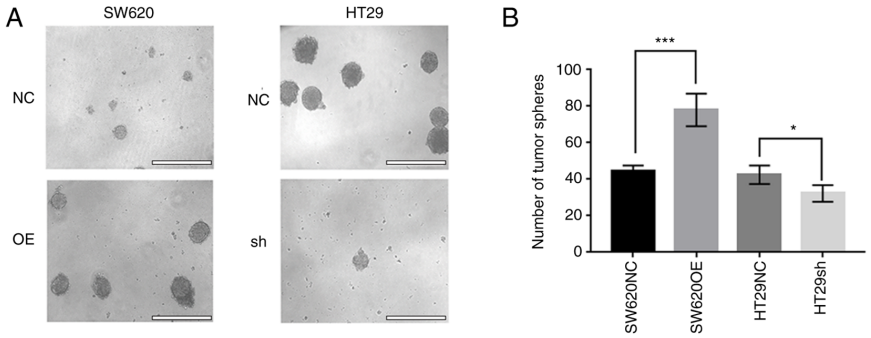


C

| Phenotype of cells | Number of cells injected | No. tumors/No. injection |
|---|---|---|
| SW620NC | $1\times10^6$ | 3/3 (100%) |
| | $1\times10^5$ | 2/3 (66.7%) |
| | $1\times10^4$ | 0/3 (0%) |
| SW620OE | $1\times10^6$ | 3/3 (100%) |
| | $1\times10^5$ | 3/3 (100%) |
| | $1\times10^4$ | 1/3 (33.3%) |

| Phenotype of cells | Number of cells injected | No. tumors/No. injection |
|---|---|---|
| HT29NC | $1\times10^6$ | 3/3 (100%) |
| | $1\times10^5$ | 3/3 (100%) |
| | $1\times10^4$ | 1/3 (33.3%) |
| HT29sh | $1\times10^6$ | 3/3 (100%) |
| | $1\times10^5$ | 1/3 (33.3%) |
| | $1\times10^4$ | 0/3 (0%) |

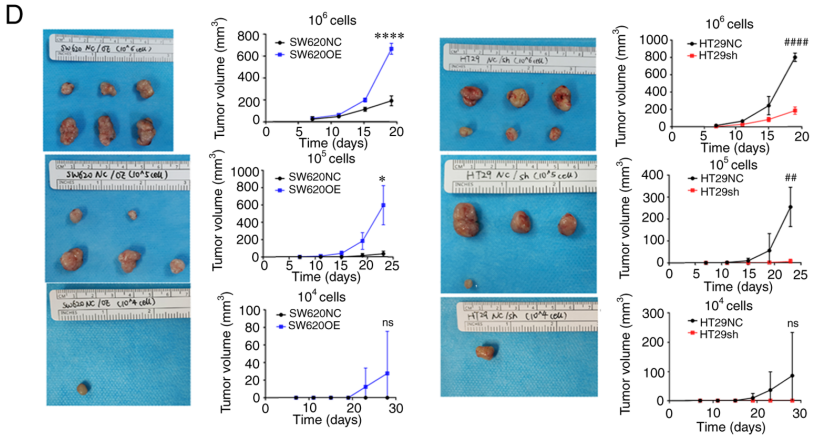


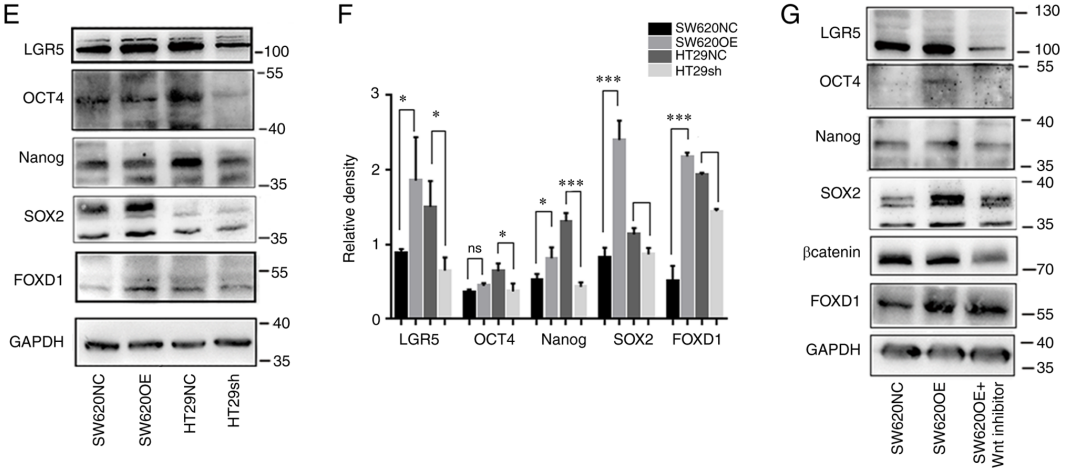


Figure 3. (A and B) Tumor sphere formation was assessed to determine the cell stemness of SW620 and HT29 cells. There were more spheroids in the SW620OE group, and less in the HT29 sh-FOXD1 group compared with in the NC groups. Scale bar, 400 $\mu$m. $^{*}$P<0.05, $^{***}$P<0.001. (C) FOXD1 OE promotes tumor-initiating capacity *in vivo*, whereas FOXD1 depletion reduces it, as analyzed by a limiting dilution assay. (D) Difference in subcutaneous tumor volume between the SW620NC and SW620OE groups, and between the HT29NC and HT29sh groups in the limiting dilution assay. $^{*}$P<0.05, $^{****}$P<0.0001 vs. SW620NC; $^{\#\#}$P<0.01, $^{\#\#\#\#}$P<0.0001 vs. HT29sh. (E) Western blot analysis and (F) semi-quantification of the expression of stemness markers in SW620OE and HT29 sh-FOXD1 cells. (G) Western blot analysis of the expression of stemness markers in SW620OE cells treated with XAV-939. $^{*}$P<0.05, $^{***}$P<0.001. FOXD1, forkhead box D1; LGR5, leucine rich repeat containing G protein-coupled receptor 5; NC, negative control; OE, overexpression; sh, short hairpin; ns, not significant.

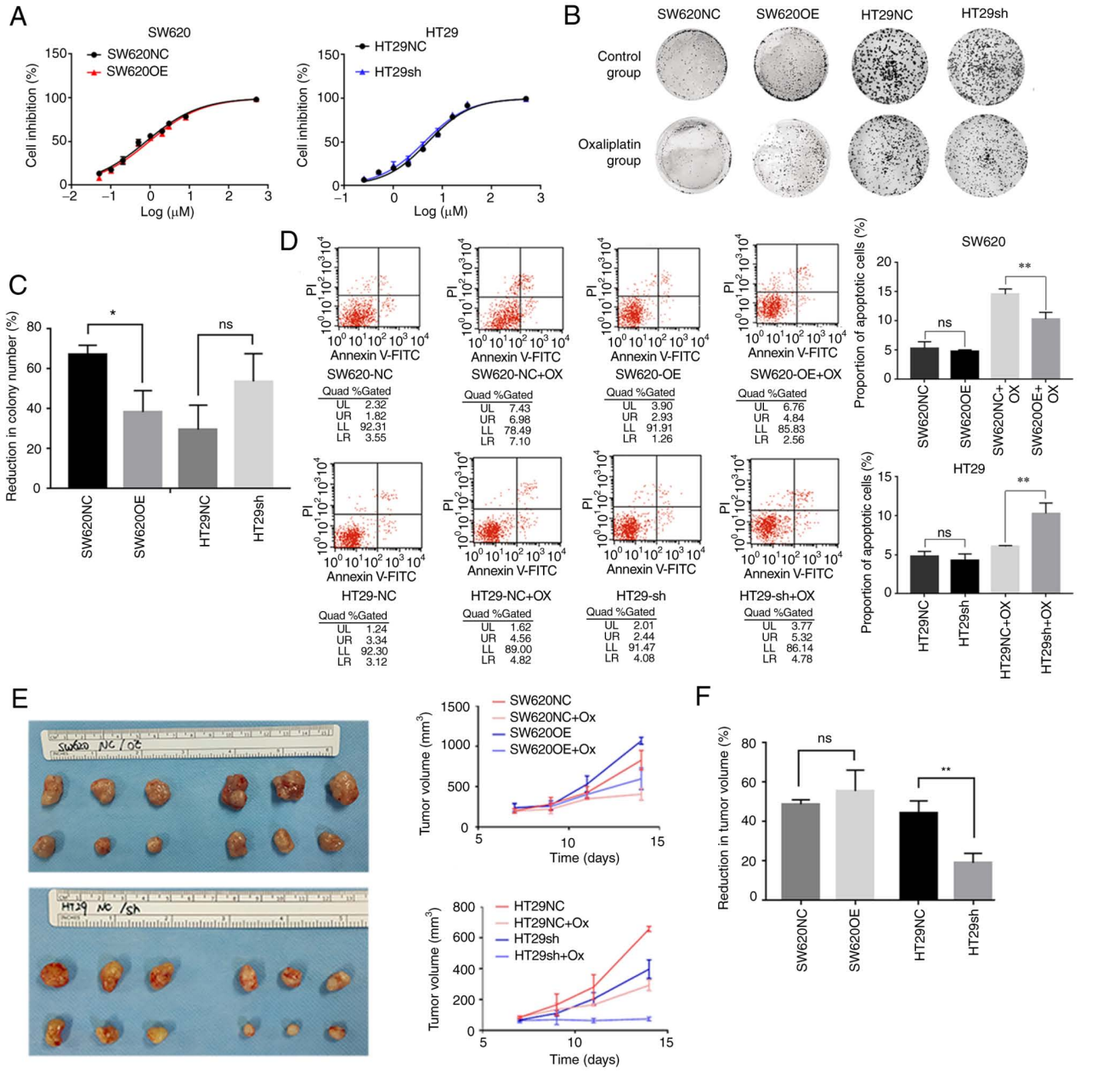


Figure 4. (A) Oxaliplatin $IC_{50}$ in FOXD1 OE SW620 cells and sh-FOXD1 HT29 cells. (B) Colony formation assay of SW620OE and HT29 sh-FOXD1 cells co-cultured with oxaliplatin compared with the NC groups. (C) Reduction in colony number (%) was determined using the following calculation: (1-number of colonies after oxaliplatin treatment/number of colonies control) x100. (D) Proportion of apoptotic cells in oxaliplatin-treated SW620OE and HT29 sh-FOXD1 cells compared with the NC groups. (E) Representative images of tumors in nude mice after various treatments. Normalized tumor growth curve indicates that FOXD1 significantly increased the chemoresistance to oxaliplatin treatment *in vivo*. (F) Reduction in tumor volume (%) was determined using the following calculation: tumor volume after oxaliplatin treatment/tumor volume of control x100. $^{*}$P<0.05, $^{**}$P<0.01. FOXD1, forkhead box D1; NC, negative control; OE, overexpression; sh, short hairpin; ns, not significant.

knockdown in the HT29sh group, a marked reduction in tumor volume occurred relative to the HT29NC group. By contrast, the tumors in the SW620OE group were markedly larger than those in the SW620NC group, and although the percentage of tumor reduction was not statistically different, a marked increase in tumor volume was detected in SW620OE groups both with and without oxaliplatin treatment (Fig. 4E and F). Reduction in tumor volume (%)=volume of tumor after oxaliplatin treatment/volume of tumor control x100.

*FOXD1 interacts directly with β-catenin to promote nuclear translocation*. IF analysis of β-catenin in each group revealed that FOXD1 promoted β-catenin nuclear translocation (Fig. 5A). To further confirm this finding, western blot analysis was performed; the results demonstrated that the overexpression of FOXD1 in SW620 cells promoted β-catenin nuclear translocation, whereas the opposite results were observed in sh-FOXD1-transduced HT29 cells (Fig. 5D and E). Co-IP is a method used to study protein interactions based on the specificity of the interaction between antibodies and antigens. It is used to determine the physiological interaction of two proteins within an intact cell. When cells are lysed under non-denaturing conditions, a number of the protein-protein interactions present in intact cells are retained. The present study performed

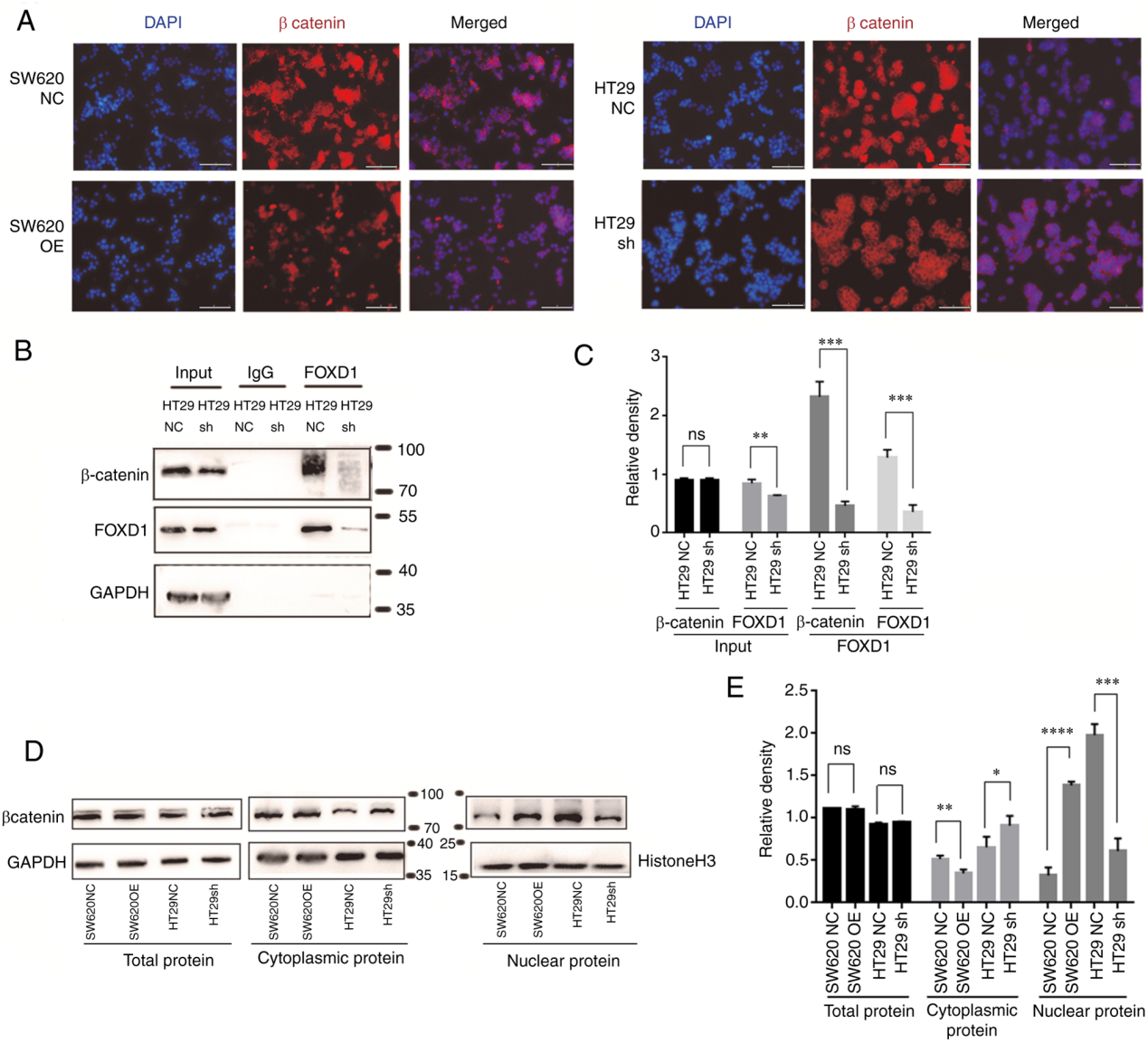


Figure 5. (A) Immunofluorescence staining of β-catenin (red) and nuclei (DAPI, blue) was performed in SW620OE cells, HT29 sh-FOXD1 and NC cells. Scale bar, 200 $\mu$m. (B) HT29 sh-FOXD1 and NC cells were subjected to co-immunoprecipitation using FOXD1 antibody or control IgG, followed by western blotting with β-catenin and FOXD1 antibodies. (C) Semi-quantification of western blotting protein bands. (D) Cytoplasmic and nuclear levels of β-catenin in SW620OE cells, HT29 sh-FOXD1 and NC cells were detected by western blotting and (E) were semi-quantified. $^{*}$P<0.05, $^{**}$P<0.01, $^{***}$P<0.001, $^{****}$P<0.0001. FOXD1, forkhead box D1; NC, negative control; OE, overexpression; sh, short hairpin; ns, not significant.

IP using an antibody against the protein FOXD1 and demonstrated that the protein β-catenin was expressed in the protein precipitate following anti-FOXD1 adsorption. Moreover, IP was performed using anti-FOXD1 on proteins extracted from HT29sh cells, and the expression of β-catenin in the protein precipitate following anti-FOXD1 adsorption was reduced compared with that in proteins extracted from HT29NC cells (Fig. 5B and C). Therefore, it was concluded that FOXD1 could bind directly with β-catenin in tumor cells and could promote β-catenin nuclear translocation.

*FOXD1 activates the Wnt/β-catenin signaling enhances EMT.* IF and western blot analyses demonstrated that FOXD1 overexpression decreased the expression levels of E-cadherin, and increased the expression levels of vimentin and N-cadherin, whereas FOXD1 knockdown decreased the expression levels of vimentin and N-cadherin, and increased the expression levels of E-cadherin (Fig. 6A-E). EMT is a reversible cellular program that transiently places epithelial cells into quasi-mesenchymal cell states. During this process, epithelial cells progressively lose their cobblestone epithelial appearance in monolayer cultures to adopt a spindle-shaped, mesenchymal morphology (21). Upon activation of EMT, E-cadherin expression is suppressed, which leads to the loss of the typical polygonal, cobblestone morphology of epithelial cells. In the present study, the FOXD1-overexpressing SW620 cells acquired a spindle-shaped mesenchymal morphology. By contrast, sh-FOXD1-transduced HT29 cells exhibited a more cobblestone-like shape, characteristic of epithelial cells (Fig. 6F).

*FOXD1 promotes tumorigenicity and tumor metastasis in vivo.* In order to verify the promoting effect of FOXD1 on CRC cells *in vivo*, stably transduced SW620 and HT29 cells were subcutaneously injected into nude mice and the subcutaneous tumor

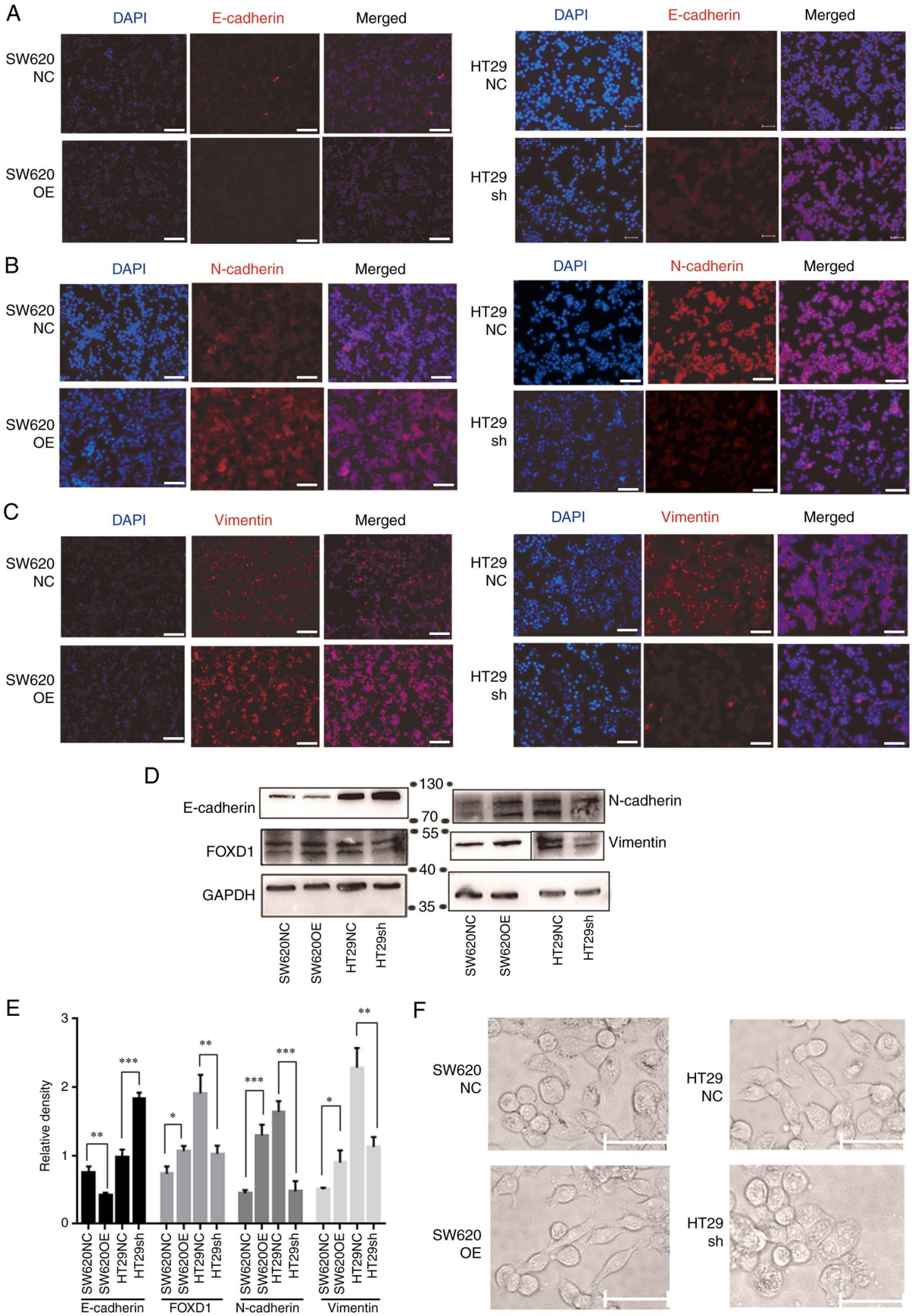


Figure 6. Immunofluorescence staining showed changes in the expression of EMT-associated proteins: (A) E-cadherin, (B) N-cadherin and (C) vimentin (red) in SW620OE cells, HT29 sh-FOXD1 and NC cells. Nuclei were counterstained with DAPI (blue). Scale bar, 200 $\mu$m. (D) Western blot analysis and (E) semi-quantification of the expression of EMT markers in FOXD1 overexpression SW620OE cells, HT29 sh-FOXD1 and NC cells. The protein expression levels of vimentin for each group were detected on the same membrane, sharing the same loading control but different exposure times. (F) Morphological changes of SW620 cells transduced with FOXD1 OE or NC vectors, and of HT29 cells transduced with sh-FOXD1 or NC vectors. Scale bar, 100 $\mu$m. $^{*}$P<0.05, $^{**}$P<0.01, $^{***}$P<0.001. FOXD1, forkhead box D1; NC, negative control; OE, overexpression; sh, short hairpin.

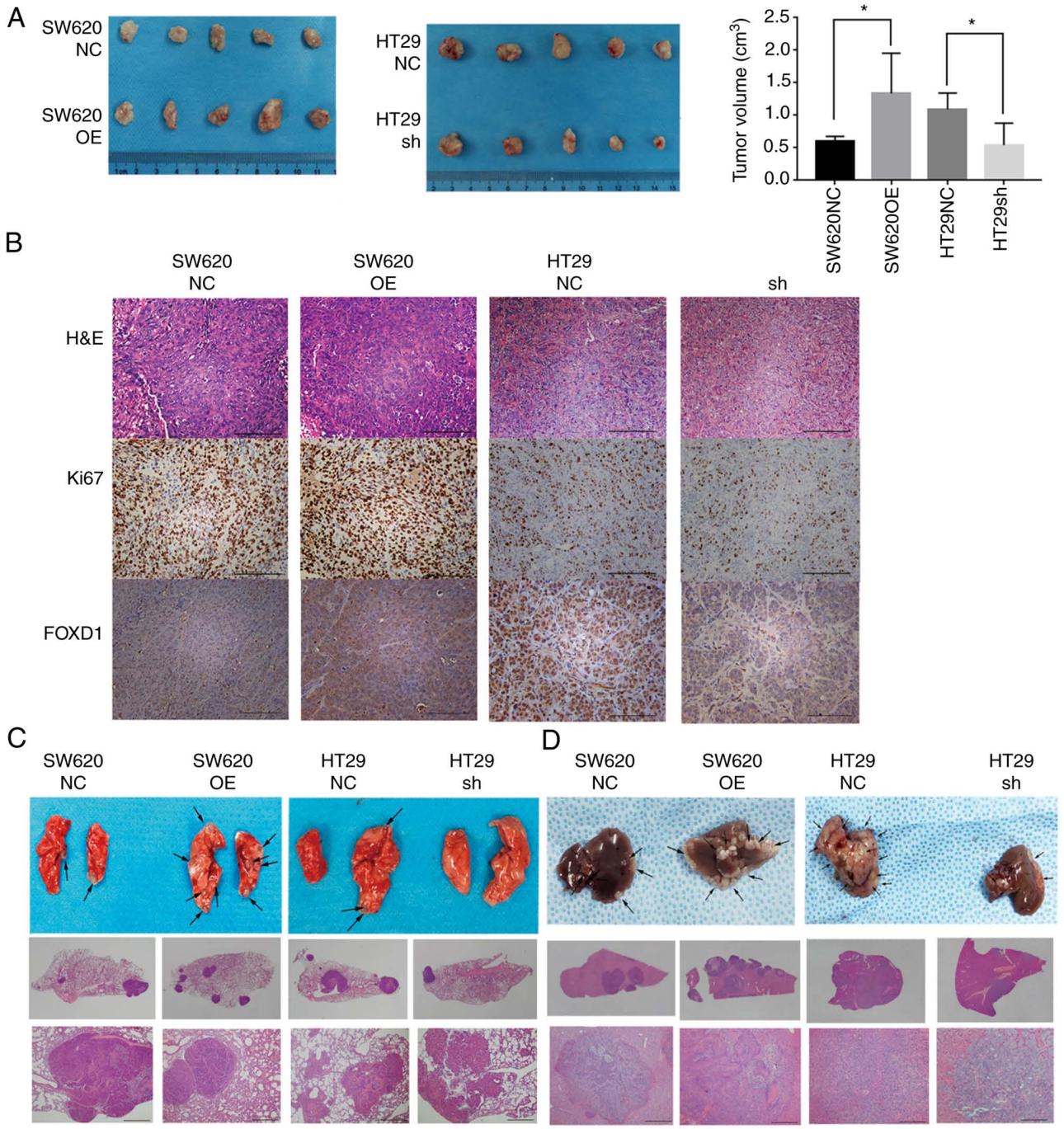


Figure 7. (A) Comparison of subcutaneous tumor growth and tumor volume after 2 weeks in xenografted nude mice, Scale bar, 200 $\mu$m. (B) H&E staining and immunohistochemical staining of subcutaneous tumors in each group of xenografted nude mice. (C) Gross and H&E staining of pulmonary metastatic nodules. Scale bar, 500 $\mu$m. (D) Gross and H&E staining of liver metastatic nodules. *P<0.05. Scale bar, 500 $\mu$m. FOXD1, forkhead box D1; H&E, hematoxylin and eosin; NC, negative control; OE, overexpression; sh, short hairpin.

growth in the xenograft nude mouse model was evaluated. FOXD1 overexpression increased tumor growth *in vivo*, whereas FOXD1 knockdown markedly suppressed tumor growth *in vivo* compared with the controls (Fig. 7A and B). Lung metastasis models were induced by injecting stably transfected cells into the tail vein of mice to examine the effect of FOXD1 on tumor metastasis. The metastatic nodules in the lungs 4 weeks after injection were examined by H&E staining. Both the quantity and size of pulmonary metastatic nodules were increased in the FOXD1-overexpression groups and decreased in the FOXD1-knockdown groups compared with in the control groups (Fig. 7C). In addition, the results of the mouse liver metastasis model revealed that knockdown of FOXD1 reduced the number of liver metastatic nodules, whereas overexpression of FOXD1 increased the number of liver metastatic nodules (Fig. 7D). These results indicated that FOXD1 may serve a critical role in tumorigenesis and tumor metastasis *in vivo*.

## Discussion

At present, surgical resection remains the most effective treatment for patients with CRC. Although the survival of patients

with CRC has been prolonged in recent years with advances in chemotherapy and radiotherapy, tumor metastasis is an important detrimental factor in the treatment and prognosis of patients with CRC (22).

At present, for patients who are resistant to conventional anticancer treatment, chemotherapy and radiotherapy have poor efficacy, and tumor progression usually results in tumor-related death within 1 year of treatment (23). As a result, there is a need to further explore novel molecular biomarkers to identify patients at high risk of metastasis and chemotherapy drug resistance, to predict clinical outcomes and to develop molecularly targeted therapeutic approaches. EMT and stemness, which drive CRC cell invasion and metastatic spread from the primary tumor, have been established as key factors in tumor development and progression (24). Increasing evidence has suggested a positive role for FOXD1 in various epithelial malignancies, and FOXD1 has been reported to be associated with aggressive occurrence and progression of lung cancer and CRC (4,25). A previous study demonstrated that FOXD1 can regulate lung cancer cell apoptosis and cell cycle via the Gal-31 regulatory loop (4). Previous studies (4,25-27) have also indicated that FOXD1 serves a role in self-renewal and tumorigenicity in mesenchymal glioma cells and breast cancer cells. The present results demonstrated that FOXD1 expression was higher in CRC tissues than in normal colorectal tissues, and it was positively associated with CRC proliferation, migration and invasion, thus indicating that FOXD1 may act as a potential biomarker to predict prognosis and metastasis in CRC.

Cell stemness is considered to be the basis of aggressive tumors (27), reflecting self-renewal and pluripotent differentiation in tumor cells, which may lead to pathogenicity, resistance to treatment, recurrence and metastasis (21). Increasing studies have identified various cancer cell types that have stem cell-like characteristics, which enhance the resistance of tumors to treatment (28,29). Therefore, targeting cancer cell stemness in CRC has become a frontier in cancer therapy. The present study revealed that the overexpression of FOXD1 promoted cell stemness in CRC, which might be the basic reason for chemotherapy drug resistance. Furthermore, the present study indicated that FOXD1-activated β-catenin may promote the EMT of CRC cells, while increasing metastasis in CRC.

There has been a wealth of research on aberrant activation of the Wnt/β-catenin pathway; almost all cases of sporadic CRC are associated with abnormal Wnt/β-catenin signaling, the activation of which increases β-catenin nuclear translocation and β-catenin forms a complex with T-cell factor/lymphoid enhancer factor to mediate target gene expression (30). Among them, β-catenin nuclear translocation is one of the most critical steps activating the Wnt/β-catenin signaling pathway (31). The present study revealed that FOXD1 enhanced the nuclear localization and transcriptional activity of β-catenin through binding to β-catenin, thus promoting cell stemness, which can make cells more resistant to chemotherapy. In addition, the Wnt/β-catenin pathway inhibitor, XAV-393, through the depletion of β-catenin, could reverse the expression of stemness markers (such as Sox2, Oct4, Nanog and LGR5) induced by enhanced FOXD1 expression. In summary, these results demonstrated that FOXD1 promoted chemotherapy resistance via enhancing cell stemness by controlling β-catenin nuclear localization.

In conclusion, the present study identified a promising cell stemness and chemotherapy resistance-associated therapeutic gene, FOXD1. The present study revealed that FOXD1 could interact directly with β-catenin and control β-catenin nuclear localization to facilitate cell stemness. Cells overexpressing FOXD1 exhibited oxaliplatin resistance, and *in vivo* experiments demonstrated that knockdown of FOXD1 had an oxaliplatin-sensitizing effect. According to these results, the increased expression of FOXD1 may inhibit the cell-killing capacity of oxaliplatin *in vitro* and *in vivo*. A limitation of the present study is that it did not investigate the specific mechanism of drug resistance in detail; however, the experimental results suggested the potential clinical application of FOXD1.

Taken together, these data indicated that FOXD1 may be a potential clinical target for the prediction of metastasis and could be a target for individualized drug therapy, which could prevent tumor metastasis and chemotherapeutic resistance to improve the prognosis of patients with CRC.

**Acknowledgements**

Not applicable.

**Funding**

No funding was received.

**Availability of data and materials**

The datasets used and/or analyzed during the current study are available from the corresponding author on reasonable request.

**Authors' contributions**

WF, JZ and AL made substantial contributions to the conception or design of the work; WF, YCZ, YPZ, HG, WL and YM made contributions to the acquisition and analysis of data. AL, MZ, ZQX and ZFX made contributions to the interpretation of data for the work. JZ and AL gave final approval of the version to be published. AL and MZ agreed to be accountable for all aspects of the work in ensuring that questions related to the accuracy or integrity of any part of the work are appropriately investigated and resolved. AL and MZ supervised the study. WF and JZ confirm the authenticity of all the raw data. All authors read and approved the final manuscript.

**Ethics approval and consent to participate**

This study was approved by the Institutional Review Board of Ruijin Hospital Ethics Committee (institutional approval no. 2018-07-015; Shanghai Jiao Tong University School of Medicine). Written informed consent to participate was obtained from all patients and the human tissue samples were anonymously coded.

**Patient consent for publication**

Not applicable.

## Competing interests

The authors declare that they have no competing interests.

## References


1. Siegel RL, Miller KD, Goding Sauer A, Fedewa SA, Butterly LF, Anderson JC, Cercek A, Smith RA and Jemal A: Colorectal cancer statistics, 2020. CA Cancer J Clin 70: 145-164, 2020.
2. Song M, Garrett WS and Chan AT: Nutrients, foods, and colorectal cancer prevention. Gastroenterology 148: 1244-1260. e16, 2015.
3. Zhu H: Targeting forkhead box transcription factors FOXM1 and FOXO in leukemia (review). Oncol Rep 32: 1327-1334, 2014.
4. Golson ML and Kaestner KH: Fox transcription factors: from development to disease. Development 143: 4558-4570, 2016.
5. Laissue P: The forkhead-box family of transcription factors: key molecular players in colorectal cancer pathogenesis. Mol Cancer 18: 5, 2019.
6. Nakano I: Transcription factors as master regulator for cancer stemness: Remove milk from fox? Expert Rev Anticancer Ther 14: 873-875, 2014.
7. Zong Y, Miao Y, Li W, Zheng M, Xu Z, Gao H, Feng W, Xu Z, Zhao J, Shen L and Lu A: Combination of FOXD1 and Plk2: A novel biomarker for predicting unfavourable prognosis of colorectal cancer. J Cell Mol Med 26: 3471-3482, 2022.
8. Gao YF, Zhu T, Mao XY, Mao CX, Li L, Yin JY, Zhou HH and Liu ZQ: Silencing of forkhead box D1 inhibits proliferation and migration in glioma cells. Oncol Rep 37: 1196-1202, 2017.
9. Nakayama S, Soejima K, Yasuda H, Yoda S, Satomi R, Ikemura S, Terai H, Sato T, Yamaguchi N, Hamamoto J, *et al*: FOXD1 expression is associated with poor prognosis in non-small cell lung cancer. Anticancer Res 35: 261-268, 2015.
10. Li D, Fan S, Yu F, Zhu X, Song Y, Ye M, Fan L and Lv Z: FOXD1 promotes cell growth and metastasis by activation of vimentin in NSCLC. Cell Physiol Biochem 51: 2716-2731, 2018.
11. Pan F, Li M and Chen W: FOXD1 predicts prognosis of colorectal cancer patients and promotes colorectal cancer progression via the ERK 1/2 pathway. Am J Transl Res 10: 1522-1530, 2018.
12. Lytle NK, Barber AG and Reya T: Stem cell fate in cancer growth, progression and therapy resistance. Nat Rev Cancer 18: 669-680, 2018.
13. Visvader JE and Lindeman GJ: Cancer stem cells: current status and evolving complexities. Cell Stem Cell 10: 717-728, 2012.
14. Takebe N, Miele L, Harris PJ, Jeong W, Bando H, Kahn M, Yang SX and Ivy SP: Targeting notch, hedgehog, and Wnt pathways in cancer stem cells: clinical update. Nat Rev Clin Oncol 12: 445-464, 2015.
15. Li F, Tiede B, Massagué J and Kang Y: Beyond tumorigenesis: Cancer stem cells in metastasis. Cell Res 17: 3-14, 2007.
16. Zhu CC, Chen C, Xu ZQ, Zhao JK, Ou BC, Sun J, Zheng MH, Zong YP and Lu AG: CCR6 promotes tumor angiogenesis via the AKT/NF-κB/VEGF pathway in colorectal cancer. Biochim Biophys Acta Mol Basis Dis 1864: 387-397, 2018.
17. Tirino V, Desiderio V, Paino F, De Rosa A, Papaccio F, La Noce M, Laino L, De Francesco F and Papaccio G: Cancer stem cells in solid tumors: An overview and new approaches for their isolation and characterization. FASEB J 27: 13-24, 2013.
18. Zhao J, Ou B, Feng H, Wang P, Yin S, Zhu C, Wang S, Chen C, Zheng M, Zong Y, *et al*: Overexpression of CXCR2 predicts poor prognosis in patients with colorectal cancer. Oncotarget 8: 28442-28454, 2017.
19. Zhu YY and Yuan Z: Pancreatic cancer stem cells. Am J Cancer Res 26: 894-906, 2015.
20. André T, Boni C, Mounedji-Boudiaf L, Navarro M, Tabernero J, Hickish T, Topham C, Zaninelli M, Clingan P, Bridgewater J, *et al*: Oxaliplatin, fluorouracil, and leucovorin as adjuvant treatment for colon cancer. N Engl J Med 350: 2343-2351, 2004.
21. Dongre A and Weinberg RA: New insights into the mechanisms of epithelial-mesenchymal transition and implications for cancer. Nat Rev Mol Cell Biol 20: 69-84, 2019.
22. Alberts SR, Horvath WL, Sternfeld WC, Goldberg RM, Mahoney MR, Dakhil SR, Levitt R, Rowland K, Nair S, Sargent DJ and Donohue JH: Oxaliplatin, fluorouracil, and leucovorin for patients with unresectable liver-only metastases from colorectal cancer: A north central cancer treatment group phase II study. J Clin Oncol 23: 9243-9249, 2005.
23. Argilés G, Tabernero J, Labianca R, Hochhauser D, Salazar R, Iveson T, Laurent-Puig P, Quirke P, Yoshino T, Taieb J, *et al*: Localised colon cancer: ESMO clinical practice guidelines for diagnosis, treatment and follow-up. Ann Oncol 31: 1291-1305, 2020.
24. Findlay VJ, Wang C, Watson DK and Camp ER: Epithelial-to-mesenchymal transition and the cancer stem cell phenotype: Insights from cancer biology with therapeutic implications for colorectal cancer. Cancer Gene Ther 21: 181-187, 2014.
25. Chen Y, Liang W, Liu K and Shang Z: FOXD1 promotes EMT and cell stemness of oral squamous cell carcinoma by transcriptional activation of SNAI2. Cell Biosci 11: 154, 2021.
26. Li CH, Chang YC, Hsiao M and Liang SM: FOXD1 and Gal-3 form a positive regulatory loop to regulate lung cancer aggressiveness. Cancers (Basel) 11: 1897, 2019.
27. Zhao YF, Zhao JY, Yue H, Hu KS, Shen H, Guo ZG and Su XJ: FOXD1 promotes breast cancer proliferation and chemotherapeutic drug resistance by targeting p27. Biochem Biophys Res Commun 456: 232-237, 2015.
28. Ombrato L, Nolan E, Kurelac I, Mavousian A, Bridgeman VL, Heinze I, Chakravarty P, Horswell S, Gonzalez-Gualda E, Matacchione G, *et al*: Metastatic-niche labelling reveals parenchymal cells with stem features. Nature 572: 603-608, 2019.
29. Carstens MR, Fisher RC, Acharya AP, Butterworth EA, Scott E, Huang EH and Keselowsky BG: Drug-eluting microarrays to identify effective chemotherapeutic combinations targeting patient-derived cancer stem cells. Proc Natl Acad Sci USA 112: 8732-8737, 2015.
30. Wilson MM, Weinberg RA, Lees JA and Guen VJ: Emerging mechanisms by which EMT programs control stemness. Trends Cancer 6: 775-780, 2020.
31. Hirabayashi Y, Itoh Y, Tabata H, Nakajima K, Akiyama T, Masuyama N and Gotoh Y: The Wnt/β-catenin pathway directs neuronal differentiation of cortical neural precursor cells. Development 131: 2791-2801, 2004.